

# A SUB-mW MICROMACHINED MAGNETIC COMPASS

Thierry C. Leïchlé<sup>1</sup>, Wenjing Ye<sup>2</sup>, and Mark G. Allen<sup>1</sup>

<sup>1</sup>School of Electrical and Computer Engineering

<sup>2</sup>School of Mechanical Engineering

Georgia Institute of Technology

Atlanta, GA, USA

## ABSTRACT

A low-power micromachined magnetic compass has been designed, fabricated and tested. Sensing of the external magnetic field is achieved by incorporating a permanent magnet into a micro mechanical resonator. The shift of the fundamental resonant frequency of the device is used to determine the amplitude or the direction of the external field. The resonator fabrication follows a CMOS-compatible, low temperature process, mainly based on surface micromachining of polymer layers. The fabricated device has been successfully demonstrated as an electronic compass, exhibiting a resolution of 45 degrees at  $30\mu\text{T}$ , for a 10V resonator excitation voltage. The power consumed by the resonator is on the order of 20nW. A theoretical model of the device was developed using vibration analysis and nonlinear deflection theory. Good agreement was observed between the predicted and observed behavior of the magnetic field sensor.

## INTRODUCTION

Sensing of the direction of the magnetic field of the Earth in a low power, compact format compatible with the size and power constraint of a wristwatch is of great commercial interest. Although a number of micromachined sensors sufficiently sensitive to sense the Earth's magnetic field have been developed, such as flux gate magnetometers and Hall-effect devices, the power requirement of these devices are typically prohibitive for a long-term, portable application [1]. Recently we proposed an alternative approach based on the use of a micromachined resonator incorporating a soft magnetic material, exhibiting a resolution of 2mT in amplitude [2]. The resonant approach is motivated by the possibility for low power excitation and the extreme sensitivity of the resonant frequency to small stresses, e.g., the stress caused by the interaction of an external magnetic field with a magnetic structure.

In this work, we present an improved device composed of a permanent magnet integrated with a rotational comb drive resonator. Improvement of the sensor sensitivity was achieved by selecting the materials and device geometry that would: (1) maximize the mechanical torque resulting from the

interaction between the external field and the magnet, and (2) emphasize its effect on the resonant frequency of the system. The fabrication of the sensor follows a CMOS-compatible process that will allow electronic excitation and sensing of the device to be done with on-chip circuitry.

## DEVICE CONCEPT

A schematic of the device is shown in Figure 1. It consists of a rotating comb drive resonator supporting a permanent magnet in its center. The structure is attached to anchor pads by means of four beams. It is actuated electrostatically by applying a voltage between two sets of comb finger electrodes. Determination of the resonant frequency is achieved by detecting the maximum rotational motion of the comb drive. In a uniform magnetic field, the interaction between the magnetization of the permanent magnet and the external field generates a torque that tends to align the direction of magnetization with the direction of the external magnetic field. The natural frequency of the rotating comb drive is sensitive to the torque produced on the magnetic portion of the resonator. The determination of the direction of the magnetic field results from the measurement of the fundamental frequency of the system. SU-8 epoxy-based resist was selected for the resonant structure because of its relatively low modulus of elasticity (resulting in very compliant beams), and its simple fabrication process, although other CMOS-compatible resonators can also be utilized. Because of its high remanent magnetization and availability in the appropriate form factor, a neodymium-iron-boron (NdFeB) permanent magnet was chosen to be integrated to the epoxy resonator.

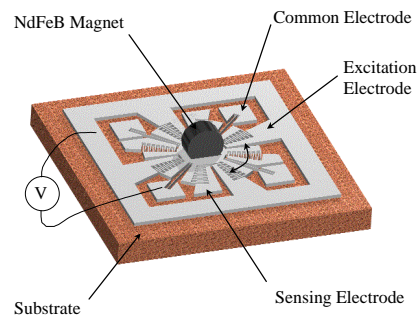


**Figure 1.** Schematic of the micromachined magnetic compass.

## THEORY

Vibration analysis and nonlinear deflection theory is used to obtain an analytical expression of the resonant frequency of the device as a function of the amplitude and direction of the external field. The interaction between an external field surrounding the sensor, shown in Figure 1, and the permanent magnet attached to the resonator produces a torque on the magnet. When the magnetization and the magnetic field are not perfectly aligned, i.e., the angle  $\mathbf{q}$  between the direction of the magnetization and the external magnetic field is different than 0 or 180 degrees, the comb drive rotates by an angle  $\mathbf{a}$  (see Figure 2). This angle is determined by solving the static equilibrium equation describing the system:

$$4k_l \mathbf{a} + 4k_n \mathbf{a}^3 - T \sin(\mathbf{q} - \mathbf{a}) = 0 \quad (1)$$

where  $k_l$  and  $k_n$ , are the linear and nonlinear stiffness coefficients of one beam, respectively. The nonlinear stiffness coefficient is introduced to account for the nonlinear load-deflection behavior of the beams when subjected to large deflections.  $T$ , the maximum amplitude of the magnetic torque, is given by equation (2) for a permanent magnet of volume  $V$  and magnetization  $M$ .

$$T = \mathbf{m}_p MVH \quad (2)$$

The expression of the fundamental resonant frequency of the sensor is obtained by solving the differential equation satisfied by the angle of vibration  $\mathbf{j}$  (equation (3)). The resonator is considered as a single degree of freedom torsional vibratory system.

$$I_{cd} \ddot{\mathbf{j}} + 4k_l (\mathbf{a} + \mathbf{j}) + 4k_n (\mathbf{a} + \mathbf{j})^3 - T \sin(\mathbf{q} - (\mathbf{a} + \mathbf{j})) = 0 \quad (3)$$

where  $I_{cd}$  is the mass moment of inertia of the comb drive. For small oscillation angles, the resonant frequency of the system is:

$$f_{cd} = \frac{1}{2p} \sqrt{\frac{4k_l + 12k_n \mathbf{a}^2 + T \cos(\mathbf{q} - \mathbf{a})}{I_{cd}}} \quad (4)$$

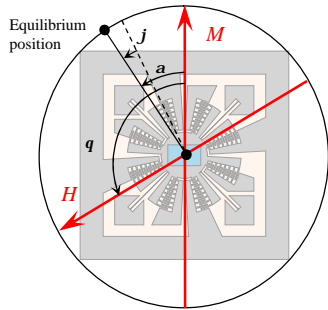


Figure 2. Top view of the device, definition of the angles.

The resonant frequency was calculated from the above theory for an epoxy structure with typical geometry values of 140 microns thickness, 2300 microns beam length, 20 microns beam width, and 2450 microns plate radius, supporting a NdFeB magnet of 900 microns diameter and 900 microns

thickness. The values of the torsional stiffness coefficients were obtained from the nonlinear behavior of a one end clamped, one end guided beam subject to large deflection presented in [3]. The static equilibrium equation was numerically solved for variable directions and amplitudes of the external field. Finally, the change of resonant frequency of the magnetic field sensor was obtained by substituting the values of the stiffness coefficients and the static angle of rotation into equation (4). Figure 3, on the left, shows the plot of the resonant frequency of the sensor as a function of the amplitude of the magnetic field for different orientations. The change of resonant frequency according to the direction of the external field can be seen on the right for several amplitudes of the applied field.

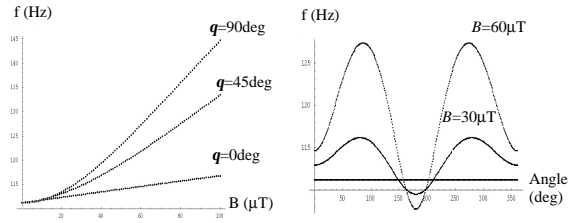
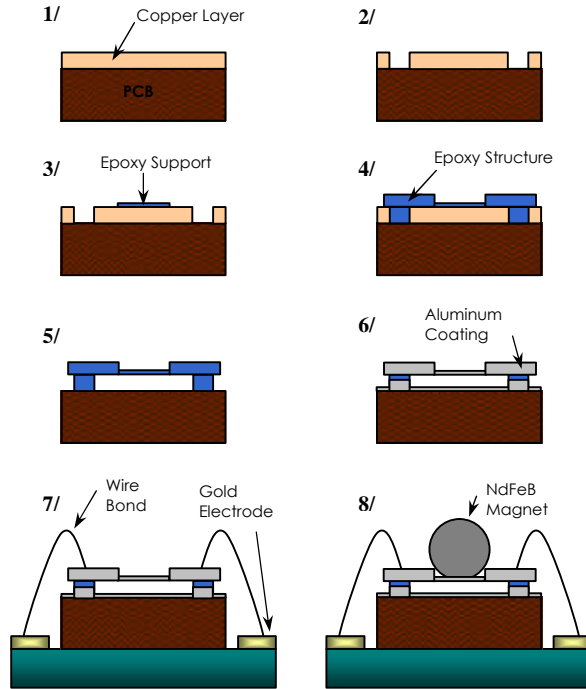


Figure 3. Variation of the resonant frequency as a function of the amplitude and the direction of the magnetic field.

## FABRICATION

The details of the fabrication process are shown in Figure 4. The substrate is a printed circuit board covered by a 70 $\mu\text{m}$  thick copper layer. The copper layer is patterned using conventional positive photoresist and is wet etched to create the anchor points for the epoxy structure. A 10 $\mu\text{m}$  layer of photosensitive epoxy is spun, cured and patterned on top of the copper layer to serve as a mechanical support for the magnet. Another epoxy layer of 140 $\mu\text{m}$  is processed to create the resonant structure. The dicing of the substrate is done before the release of the resonators because of the lower risk to break the devices. The copper sacrificial layer is then wet etched to release the suspended parts of the epoxy structures. The resonators are conformally coated with 300nm of aluminum to create conductive electrodes at the surface of the devices. To facilitate the test of the sensor, each diced device is glued to a glass substrate, on which gold electrodes were previously patterned for electrical connections. A lapper is used to make a flat on the curved surface of a cylindrical NdFeB magnet, allowing the magnet to sit vertically. The magnet is then manually glued on the top of the resonator. The patterning of the second layer of epoxy is used as a guide for the magnet positioning. Figure 5 shows a completed sensor ready for testing. The sensor incorporates a gold-coated NdFeB permanent magnet.



**Figure 4.** Fabrication process of the compass: 1/Polishing of the copper layer; 2/After patterning of the anchor pads; 3/Creation of the support for the magnet; 4/Fabrication of the epoxy structure; 5/Release of the resonator; 6/Conformal coating; 7/Packaging; 8/Mounting of the permanent magnet.

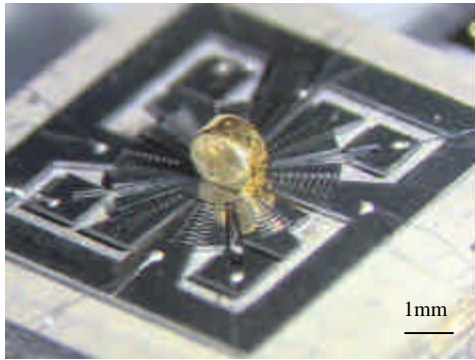


**Figure 5.** Photograph of a fabricated epoxy structure incorporating a gold-coated permanent magnet.

## MEASUREMENTS AND RESULTS

Functional devices have been successfully fabricated and tested. Measurement of the fundamental resonant frequency of the comb drive resonator has been achieved optically and electrically. Optical measurement of the resonant frequency was done by determining the maximum angular deflection of the comb drive with an optical microscope. Electrical detection was achieved by measuring the peak of current intensity flowing through the comb drive at the third harmonic of the excitation signal. For magnetic sensing assessment, the device was placed in the vicinity of a coil that generated a magnetic field

in the plane of the resonator. Variation of the intensity of the magnetic field was achieved by controlling the current flowing through the coil. The angle of the sensor relative to the field could be varied using the rotating stage of the microscope. The applied magnetic field was independently measured by means of an external FwBell9550 Gaussmeter.

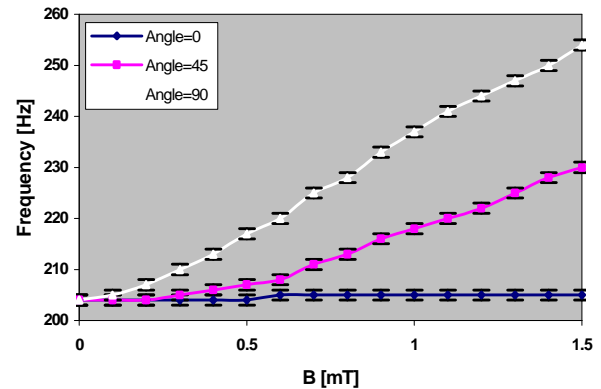


**Figure 6.** Resonant frequency of a first sensor as a function of the magnetic field intensity. The angle between the direction of the field and the magnetization is set to  $0^\circ$ ,  $45^\circ$ , and  $90^\circ$ .

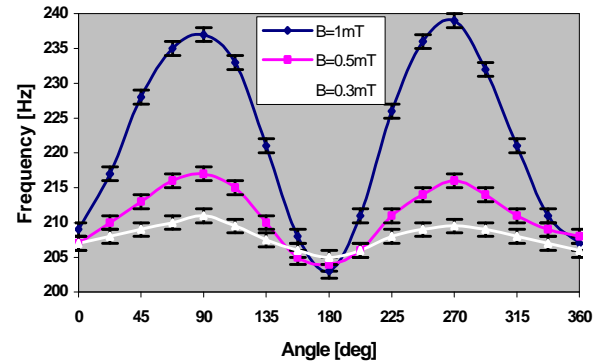


**Figure 7.** Resonant frequency of the first sensor as a function of the direction of the magnetic field. An angular orientation of  $0^\circ$  indicates that the applied magnetic field is parallel to the direction of magnetization of the magnet. The field intensity is set to 0.3mT, 0.5mT, and 1mT.

The resonant frequency was measured as a function of the amplitude of the incident magnetic field. Figure 6 shows the variation of the resonant frequency of a first device as a function of the applied induction for different angles between the direction of the field and the magnetization of the permanent magnet. Resonant frequency was determined using the optical method. The dependence of the resonant frequency on the rotational angle between the applied magnetic field and the magnetization was also investigated. It is given in Figure 7 for the same device. The dependence of resonant frequency was plotted for three different values of the magnetic field excitations.

The behavior of a device exhibiting a lower resonant frequency was also studied. The device was excited using an AC signal of 37.5V. No magnetic field was applied, thus allowing the sensor to determine the direction of the Earth's magnetic field. Figure 8 shows the dependence of the resonant frequency on the rotational angle. A minimum resolution of 10deg in the direction of the field was estimated from the plotted results. Resolution in the amplitude of the field is expected to be well below 30 $\mu$ T, but is difficult to quantify from the current experimental data. The same experiment, conducted with an excitation voltage of 10V, showed that sensor has the ability to determine the main directions of the Earth's magnetic field (with a 45deg resolution) at low excitation voltages. The estimated power consumption of the device was then 20nW.

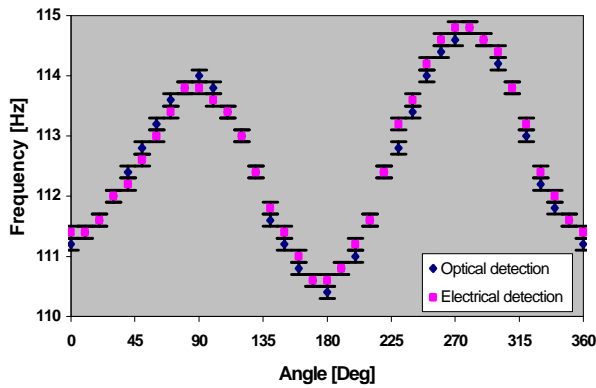


**Figure 8.** Resonant frequency of a 109Hz natural frequency sensor as a function of the orientation of the sensor relative to the Earth's magnetic field. No additional external magnetic field is applied.

## DISCUSSION

The experimental resonant frequencies shown in Figure 8 are close enough to the theoretical values to allow us to fit the data with the theoretical model and to deduce empirical values for the magnetic torque and the stiffness coefficients of the beams. The theory predicts that there will be a difference in resonant frequency for an angular orientation between sensor and external magnetic field  $q$  of zero and 180 degrees, depending on the magnitude of the external torque and the linear stiffness coefficient. The measured values of resonant frequency at values of  $q$  are therefore used to determine these two quantities. The deduced torque of  $1.2 \times 10^{-8}$ Nm is lower than the theoretical value used in the model ( $5.2 \times 10^{-8}$ Nm), most likely due to demagnetization effects causing an overestimation of the remanent magnetization of the NdFeB permanent magnets, as well as potential damage to the magnet during its preparation for mounting. The empirical value of the linear stiffness

coefficient of the beams correlates very well with the theoretical prediction (both values are about  $4.1 \times 10^{-7}$  Nm). The variation of the resonant frequency of the sensor as a function of  $q$  was estimated for different nonlinear stiffness coefficients using equation (4) and the empirical values previously obtained. Figure 9 shows a plot giving the experimental and empirical resonant frequencies as a function of the direction of the magnetic field. Estimation of the most accurate fit of the theoretical plot led to the empirical value of the nonlinear coefficient of the beams. The empirical nonlinear stiffness coefficient is found to be larger than the calculated coefficient ( $1.75 \times 10^{-4}$ Nm vs.  $1.37 \times 10^{-5}$ Nm). This may be due to the relatively simple assumptions used to describe the nonlinearities inherent in the device.

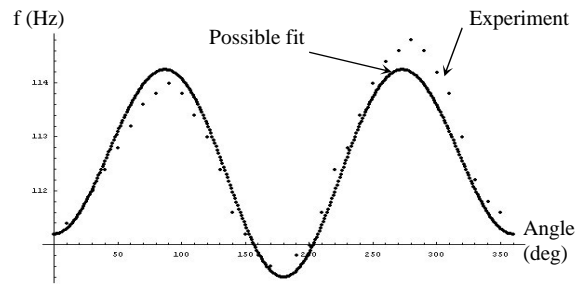


**Figure 9.** Experimental and empirical resonant frequencies as a function of the direction of the magnetic field.

## CONCLUSION

We designed, fabricated and tested a micromachined comb drive resonant magnetic field sensor incorporating a permanent magnet. The device has been successfully used as an electronic compass. Operated at low voltage (10V) and consuming very low power (20nW), the sensor can resolve 45 degrees in the determination of the direction of the Earth's magnetic field. We developed a theoretical model predicting the change of resonant frequency of the resonator as the direction or the magnitude of the external field varies. The model showed good agreement with experimental results.

## REFERENCES

- [1] J. E. Lenz, "A review of magnetic sensors", *Proceedings of the IEEE*, vol.78, no.6, June 1990, pp.973-89.
- [2] T. C. Leïchl , M. von Arx, and M. G. Allen, "A Micromachined Resonant Magnetic Field Sensor", *Proceedings IEEE Micro Electro Mechanical Systems*, Interlaken, Switzerland 21-25 January 2001.
- [3] R. Legtenberg, A. W. Groeneveld, and M. Elwenspoek, "Comb-drive actuators for large displacements", *J. Micromech. Microeng.* 6 (1996) 320-329.